



University of HUDDERSFIELD

University of Huddersfield Repository

Li, Y., Tian, Gui Yun and Cui, Z.

Theoretical and experimental study on magnetically-actuated micromirrors for electromagnetic NDE

Original Citation

Li, Y., Tian, Gui Yun and Cui, Z. (2006) Theoretical and experimental study on magnetically-actuated micromirrors for electromagnetic NDE. In: Proceedings of Computing and Engineering Annual Researchers' Conference 2006: CEARC'06. University of Huddersfield, Huddersfield, pp. 1-6.

This version is available at <http://eprints.hud.ac.uk/id/eprint/3805/>

The University Repository is a digital collection of the research output of the University, available on Open Access. Copyright and Moral Rights for the items on this site are retained by the individual author and/or other copyright owners. Users may access full items free of charge; copies of full text items generally can be reproduced, displayed or performed and given to third parties in any format or medium for personal research or study, educational or not-for-profit purposes without prior permission or charge, provided:

- The authors, title and full bibliographic details is credited in any copy;
- A hyperlink and/or URL is included for the original metadata page; and
- The content is not changed in any way.

For more information, including our policy and submission procedure, please contact the Repository Team at: E.mailbox@hud.ac.uk.

<http://eprints.hud.ac.uk/>

THEORETICAL AND EXPERIMENTAL STUDY ON MAGNETICALLY-ACTUATED MICROMIRRORS FOR ELECTROMAGNETIC NDE

Y. Li¹, G. Y. Tian¹ and Z. Cui²

¹ University of Huddersfield, Queensgate, Huddersfield HD1 3DH, UK

² Central Microstructure Facility, Rutherford Appleton Laboratory, Chilton, Didcot OX11 0QX, UK

ABSTRACT

Magnetically-actuated Micromirrors as Micro-electromechanical devices have exhibited their superiority over other magnetic sensing techniques in terms of high sensitivity and high spatial resolution, which is favoured not only by quantitative measurement but also imaging of magnetic field distribution. In our research into magnetic field sensing and imaging, a 2D magnetic field sensing system with magnetically-actuated micromirrors has been proposed. Before the system is constructed, extensive investigation of magnetically-actuated micromirrors with different structures and materials has been conducted via theoretical and experimental study. FEMLAB and IntelliSuite have been employed for theoretical analysis of the sensitivity of micromirrors with different structures in correlation with the variation of external magnetic fields in order to optimise micromirror dimensions and beam cantilever design. Following the innovative fabrication of practical micromirrors, an optical measurement system has been set up to specifically characterise micromirrors of various dimensions and configurations in terms of sensitivity to the variation of external magnetic field. Detection sensitivity of 1 deflection degree of micromirror per Gauss of magnetic field has been achieved, which benefits not only the further improvement of micromirror sensitivity via optimal design and fabrication, but also the establishment of a micromirror-based 2D magnetic field sensing and imaging system for ENDE with high sensitivity and high spatial resolution.

Keywords MEMS, Magnetic force, Magnetically actuated micromirror, Magnetic sensor, NDE

1 INTRODUCTION

Because electromagnetic signals contain a wealth of information on the integrity of conductive specimens under inspection, magnetic field sensing and imaging play a vital role in Electromagnetic Nondestructive Evaluation (ENDE). Besides traditional coils and coil arrays used in ENDE, solid-state magnetic field sensors have already been extensively employed in laboratory-based research as well as routine industrial inspection^[1-5]. Although the application of solid state devices fulfils the requirements of magnetic field sensing with relatively high sensitivity, they experience low-spatial-resolution and time-consuming problems. Even though there have been recent breakthroughs in magnetic field imaging techniques in pursuit of high spatial resolution, e.g. magneto-optical imaging techniques^[6], they suffer from low sensitivity and high implementation cost. Therefore, the development of relatively low cost magnetic field sensing and imaging for ENDE with high sensitivity and spatial resolution remains a challenge.

Micromirrors, as a member of Micro-electromechanical systems (MEMS)^[7], are widely used for delicate sensors, actuators and sensing systems in various areas, which traditionally convert an electrical signal into a mechanical output. The deflection of micromirrors is measured by using appropriate systems such as optical systems^[8-10]. As an alternative to electrostatic and piezoelectric actuation, magnetic actuation has shown promise in the detection and quantification of magnetic fields and has the advantage that magnetic actuation by either repulsive or attractive magnetic forces in a microactuator can be large^[11]. In addition, the well-established magnetic thin-film head technology^[12, 13] essentially benefits the development of magnetically-actuated micromirrors (MAMs).

Fabrication of micromirrors or microcantilevers has been widely reported. Surface micromachining is the most popular way of making such micromechanical structures^[14]. It involves deposition of polysilicon or silicon nitride thin film on top of a sacrificial layer. Subsequent removal of the sacrificial layer releases the cantilevers or micromirrors to allow them free mobility under external forces. Surface micromachining has problems in depositing a stress free thin film and releasing cantilevers.

In a bid to measure the disturbance in magnetic field caused by defects in conductive materials, a novel Magnetically Actuated Micromirror (MAM) is to be designed via theoretical and experimental study, fabricated with innovative techniques and applied to ENDE of specimen integrity.

2 THEORETICAL STUDY

Basically, MAM consists of a relatively large mirror plate which comprises magnetic permalloy^[15, 16] electroplated on a substructure plate, and suspended beams which anchor the mirror plate to a supporting frame. The deflection of a MAM is directly proportional to the magnetic force exerted on the mirror plate, which is expressed in Equation (1) as function of magnetic properties as well as dimensions of the mirror plate^[17, 18]:

$$F = V_{mag} |\overline{M} \times \overline{H}| = V_{mag} MH \sin \alpha \quad (1)$$

where, V_{mag} and \overline{M} denote respectively the volume and magnetisation vector of magnetic permalloy.

\overline{H} is the external magnetic field intensity and α denotes the angle between \overline{M} and \overline{H} .

The MAM design started with a theoretical investigation of the deflection of the MAM against different intensities of externally applied magnetic field by solving Equation (1) analytically or numerically. Instead of employing analytical models proposed in Reference [18], a completely different design methodology has been developed. Not only the magnetic force on mirror plate but also the dimension and configuration of suspended beams have been analysed via Finite element simulation (FEM). 3D FEM models were built up and simulated in commercial simulation packages i.e. FEMLAB^[19] and IntelliSuite^[20] to derive the relationship between the magnetic force and the MAM deflection in a static magnetic field with variable intensity. The schematic illustration of modelling is presented in Figure 1 along with Figure 2 showing the micromechanical modelling of MAM deflection in IntelliSuite under external force obtained in electromagnetic simulation conducted in FEMLAB.

Figure 3 presents the magnetic force against external magnetic field intensity for mirrors with different dimensions, which is obtained in FEMLAB. In parallel, the micromechanical simulation in IntelliSuite provides the deflection of suspension beam against different beam lengths with respect to particular mirror size and magnetic force, which is exhibited in Figure 4. From the simulation results presented in Figures 3 and 4, it can be seen that the correlation of magnetic force with external magnetic field is quadratic in manner, which indicates that the force actuating the MAM to deflect is directly proportional to the applied field. Similar conclusions can be drawn from Figure 4, in that the longer the suspension beam, the more sensitivity the MAM has to variation of the applied field. Moreover, especially from micromechanical simulations, it is revealed that the single beam anchor has the highest flexibility. However, single beam anchoring also displays torsional behaviour, which is not desirable because of the possible skewed deflection. The twin beam cantilever mirror is preferred as it can generate directional and unskewed deflection in an external magnetic field.

The theoretical study of MAM has directed the following task for MAM design. There are two factors that can influence the sensitivity of magnetic field detection: the volume of magnetic material on the mirror surface and the flexibility of suspension beam. As the magnetic force is a volume force, for a fixed magnetic field the larger the volume of magnetic material, the greater the induced magnetic force. This effect is illustrated by Figure 3. The volume of magnetic material can be increased by increasing the size of mirror plate and using thicker permalloy deposited onto the substructure plate. The flexibility of suspension beam can be improved by increasing beam length and reducing the beam cross-section, or reducing the beam rigidity. With consideration of these two factors in design, MAMs of various dimensions and configurations were designed and fabricated on a 4" wafer, following which the experimental study on the characterisation of MAM was carried out.

3 EXPERIMENTAL STUDY

3.1 Fabrication of MAMs

To fabricate the MAMs, the surface micromachining technique has been adopted, which involves deposition of a polysilicon layer on top of a sacrificial layer, and subsequent removal of the sacrificial layer to release the mirror structure so that it can be freely deflectable under an external force.

Electroplated permalloy inevitably has a rough surface and cannot serve as the mirror reflection surface. Figure 5(a) is an optical image of a mirror before permalloy electroplating. In contrast, Figure 5(b) exhibits the SEM image of a mirror after permalloy (Ni80Fe20) electroplating. The SOI wafer process offers another advantage that no other process can, that is to provide both the surface for electroplating of permalloy and the surface for mirror reflection of a laser beam. After etching through from the backside to release the mirror, the backside surface of the mirror plane is of polished surface quality and can serve very well as the mirror reflection surface. Fabricated MAMs in different geometries were assembled in chips with various configurations. Each chip can be an array of mirrors of the same geometry, or a cluster of mirrors of different dimensions.

3.2 Characterisation of MAMs

In a bid to identify the relationship between the deflection of MAMs and the externally applied magnetic field, an optical measurement system has been set up.

3.2.1 Experimental setup

Figure 7 shows the optical measurement system for MAM characterisation, which includes:

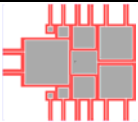

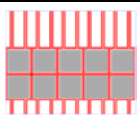
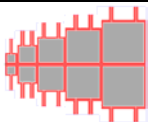
- A laser source for generation of the intensive laser beam illuminating each MAM chip;
- A permanent magnet for exerting a static magnetic field varying from 1 Gauss to 20 Gauss over the MAMs to actuate each MAM to deflect;
- A hall device underneath the plate of MAM chips to quantify the vertical component of the applied magnetic field that mostly contributes the deflection of the MAM;
- A CCD camera that outputs the image signal providing positional information for the reflected light spots with respect to a particular intensity of magnetic field.

During each measurement, the magnet was moved horizontally towards the MAM sample. The closer the magnet to the sample, the stronger the magnetic field exerted on the mirrors. The intensity of magnetic field was measured by the Hall device in real time. Each MAM chip was illuminated by the incident laser with an illuminating area of $500\mu\text{m} \times 50\mu\text{m}$ stripe. Several light spots were recorded by the CCD camera due to the reflection of laser beams from a MAM chip. Each measurement was repeated twice, i.e. one set of measurements were taken, then the sample was rotated by 90° and another set of measurements taken, corresponding to measurements in X and Y directions along the MAM chips. The displacement of light spots due to the variation of magnetic field over the MAMs, which were recorded by the CCD camera, were worked out from the analysis of a series of captured images by employing an algorithm for image processing implemented in MATLAB. The displacement of each spot is represented by pixel count in the captured image; consequently, it is an arbitrary length scale. However, from the distance between MAM plane and recording plane, as illustrated in Figure 7, the displacement can be converted into the deflection angle of the MAM by applying the fundamental trigonometric relationship within the entire system.

3.2.2 MAM chips under investigation

4 MAM chips with different configuration of MAMs were investigated. The dimensional information of each MAM is listed in Table 1 along with the illustration of each chip. The deflection of MAMs in each chip against intensity of externally applied magnetic field was obtained individually from x-direction and y-direction measurement.

Table 1. MAM chips under investigation

Chip1 [MS*: 50, 100, 200, 300, 400] [BL**: 200]	Chip4 [MS: 300] [BL: Folded]	Chip8 [MS: 300] [BL: 200, 500]	Chip9 [MS: 100, 200, 300, 400, 500] [BL: 200]
			

*MS: The length of MAM Size (unit: μm)

**BL: The length of suspension beam (unit: μm)

3.3 Experimental results and discussion

The experimental results illustrating the deflection angle of MAMs in each chip against applied magnetic field is presented in Figure 8. Figure 8(a) exhibits the results for sample 1 where the thickness of suspension beam is equal to that of MAMs. In contrast, in sample 2, the thickness of suspension beam is half of that of MAMs, the results of which are shown in Figure 8(b).

As predicted in the theoretical study, the practical relationship between MAM deflection angle and externally applied magnetic field is quadratic in manner, which indicates that the larger the magnetic field intensity, the higher the sensitivity of MAMs in the magnetic field. As can be seen in Figure 8, MAMs with larger volume of magnetic materials on mirror plates as well as longer suspension beams respond with more sensitivity to the variation of externally applied magnetic field with larger deflection angle. From Figure 8, it is noteworthy that the MAMs in Chip4 and Chip8 exhibit higher sensitivity to magnetic field change since MAMs in Chip4 and Chip8 respectively have longer and folded-structure suspension beams, compared to MAMs in other chips. Interestingly, although the MAMs in Chip1 and Chip9 have $500\mu\text{m} \times 500\mu\text{m}$ mirror plates which are the largest size of mirror, the sensitivity of Chip1

and Chip9 are still inferior to Chip4 and Chip8, which indicates that the length and structure of suspension beams are of greater importance in improving the sensitivity of MAMs.

Moreover, comparing Figure 9(a) to Figure 9(b), the sensitivity of the MAMs having smaller thickness of suspension beam is higher than those with beam thickness equal to mirror plates'. Take Chip4 for example, as shown in Figure 10, the MAMs of sample 2 exhibit much more significant response to variation of magnetic field than those of sample 1 for both x-direction and y-direction measurements. In addition, from Figure 10, it can be found the sensitivity at about 1 degree deflection per Gauss of magnetic field has been achieved by adopting the folded suspension beam with thinner thickness.

4 CONCLUSION AND FURTHER WORK

In summary, MAMs have been designed via theoretical study, and fabricated using an innovative SOI wafer process. The new process offers stress-free micromechanical structures in silicon to address the stiction problem encountered in conventional surface micromachining process when releasing mirror structures, and also makes it possible to electroplate a permalloy layer on one side of substructure plate and to maintain a mirror plate as the reflection surface on the other side.

MAMs of 13 different geometries were fabricated on a 4" SOI wafer. The fabrication technique has been proven. Valuable experience in microfabrication of these magnetic micromirrors has been acquired. These MAMs have been characterised using an optical system employing laser beam reflection and CCD camera recording. These MAMs have been proved to effectively deflect under the influence of proximity magnetic field. The measurement results have validated the computer modelling. So far for the current fabricated MAMs, detection sensitivity to variation of external magnetic field at about 1 degree deflection per Gauss magnetic field has been achieved.

There is certainly room for further improvement in detection sensitivity, for example, by increasing the thickness of permalloy layer and increasing the flexibility of suspension beam during fabrication, which are all achievable. In parallel, the dynamic characteristics of the fabricated MAMs are to be investigated with time-variant magnetic field e.g. sinusoidal field introduced in experiments. The establishment of the MAM-based 2D magnetic field sensing and imaging system for ENDE is underway.

REFERENCES

- [1] G. Y. TIAN, A. SOPHIAN, D. TAYLOR and J. RUDLIN (2005), *Multiple sensors on pulsed eddy-current detection for 3-D subsurface crack assessment*, IEE Sensors Journal, Vol. 5, No. 1, pp. 90-96.
- [2] G. Y. TIAN and A. SOPHIAN (2005), *Study of magnetic sensors for pulsed eddy current techniques*, Insight, 47(5), pp. 277-280.
- [3] A. SOPHIAN, R. S. EDWARDS, G. Y. TIAN and S. DIXON (2005), *Dual-probe methods using pulsed eddy currents and electromagnetic acoustic transducers for NDT inspection*, Insight, Vol. 47(6), pp. 341-345.
- [4] J. W. WILSON, G. Y. TIAN and S. BARRANS (2006), *Residual magnetic field sensing for stress measurement*, Sensors and Actuators A, In Press.
- [5] Y. LI, J. W. WILSON and G. Y. TIAN (2006), *Experiment and simulation study of 3D magnetic field sensing for magnetic flux leakage defect characterisation*, International NDT&E, In Press.
- [6] P.-Y. JOUBERT and J. PINASSAUD (2006), *Linear magneto-optic imager for non-destructive evaluation*, Sensors and Actuators A, Vol. 129, No. 1-2, pp. 126-130.
- [7] J. P. ZHAO, H. L. CHEN, J. M. HUANG and A. Q. LIU (2005), *A Study of Dynamic Characteristics and Simulation of MEMS torsional Micromirrors*, Sensors and Actuators, Vol. 120, pp. 199-210.
- [8] Y. OKANO and Y. HIRABAYASHI (2002), *Magnetically Actuated Micromirror and Measurement System for Motion Characteristics Using Specular Reflection*, IEEE Journal on Selected Topics in Quantum Electronics, Vol. 8, No. 1, pp. 19-25.
- [9] RAANAN A. MILLER, GEOFFREY W. BURR, YU-CHONG TAI and DEMETRI PSALTIS (1995), *Magnetically Actuated Micromirrors for use as Optical Deflectors*, Proceedings of The Electrochemistry Society Meeting, 95-18, pp. 474-480.
- [10] I. J. CHO, K-S YUN, H-K LEE, J-B YOON and E YOON (2002), *A low-voltage Two-axis Electromagnetically Actuated Micromirror with Bulk Silicon Mirror Plates and Torsion Bars*, 15th IEEE International Conference on Micro-Electromechanical Systems, pp. 540-543.

[11] J. A. WRIGHT, T. YU-CHONG and C. SHIH-CHIAN (1997), *A Large-force Fully-integrated MEMS Magnetic Actuator*, Technical Digest: 1997 International Conference on Solid-State Sensors and Actuators: Transducers '97, Vol. 2, pp. 793-796.

[12] M. VOLMER and J. NEAMTU (2003), *Computer Simulation of Magnetization Curves in Magnetic Thin Films*, J. of Optoelectronics and Advanced Materials, 5 (1), pp. 319-324.

[13] R. LOPUSNIK, J. P. NIBARGER, T. J. SILVA and Z. CELINSKI (2003), *Different Dynamic and Static Magnetic Anisotropy in Thin Permalloy Films*, Applied Physics Letters, 83 (1), pp. 96-98.

[14] H. MAHFOZ-KOTB, A.C. SALAÜN, F. BENDRIAA, F. LE BIHAN, T. MOHAMMED-BRAHIM and J.R. MORANTE (2006), *Sensing sensibility of surface micromachined suspended gate polysilicon thin film transistors*, Sensors and Actuators B, Vol. 118, No. 1-2, pp. 243-248.

[15] N. V. MYUNG, D. Y. PARK, B. Y. YOO and P. T. A. SUMODJO (2003), *Development of Electroplated Magnetic Materials for MEMS*, Journal of Magnetism and Magnetic Materials, Vol. 265, pp. 189-198.

[16] R. F. SHYU, H. YANG, C. T. PAN and P. TSAI (2005), *Hard Magnetic Material for Perpendicular Magnetic Anisotropic Field in Electromagnetic Actuator Fabrication*, Progress in Electromagnetics Research Symposium, pp. 1-5.

[17] L. CHANG and W. Y. YONG (1999), *Micromachined Magnetic Actuators Using Electroplated Permalloy*, IEEE Transactions on Magnetics, 35 (3), pp. 1976-1985.

[18] J. W. JUDY and R. S. MULLER (1997), *Magnetically Actuated Addressable Microstructures*, Journal of Microelectromechanical Systems, 6(3), pp. 249-256.

[19] INTELLISENSE (2005), *Intellisuite 8 Manual*, <http://www.intellisensesoftware.com>.

[20] COMSOL CORPORATION (2004), *FEMLAB V3.1 Manual*, <http://www.comsol.com/>.

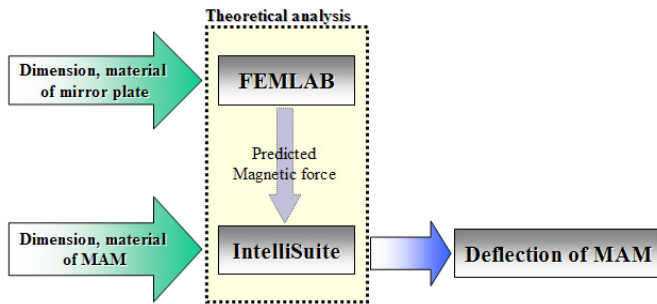


Figure 1. Schematic illustration of MAM deflection simulation

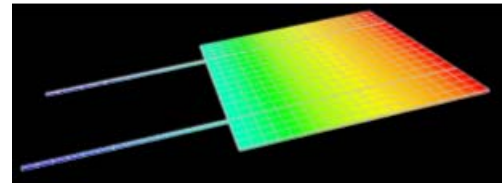


Figure 2. Micromechanical simulation of MAM

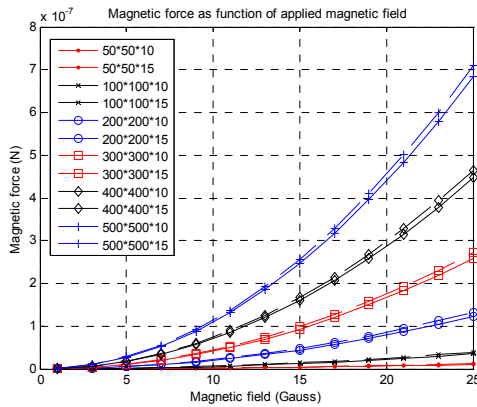


Figure 3. Magnetic force vs. external magnetic field for different mirror size

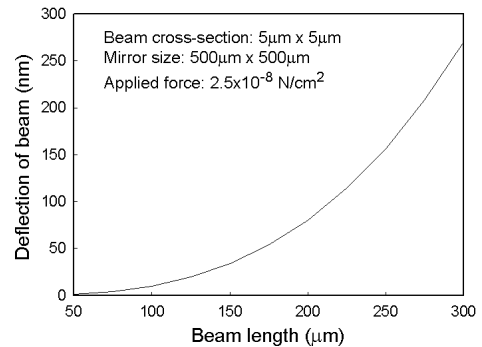
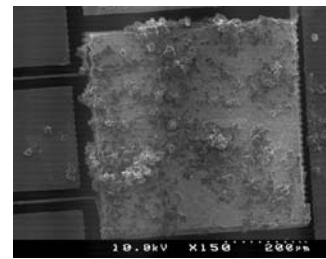


Figure 4. Deflection of suspension beam vs. beam length



(a)



(b)

Figure 5. Micromirror surface before and after electroplating of permalloy (a). Before electroplating of permalloy; (b). After electroplating of permalloy

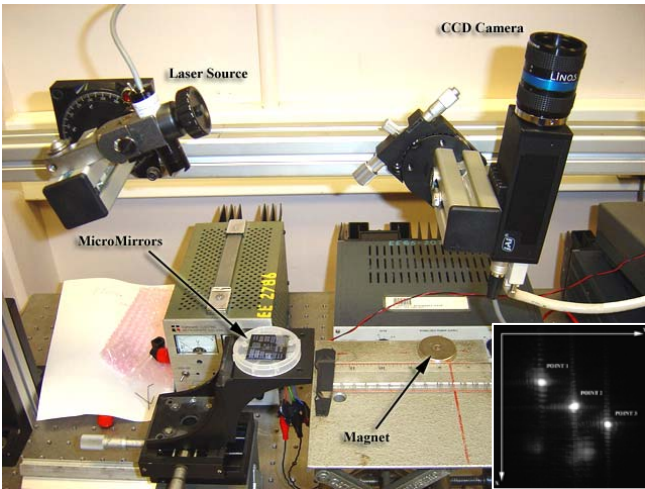


Figure 6 Experimental setup for optical measurement of MAMs (Inset: Grey-scaled image of spots from CCD camera)

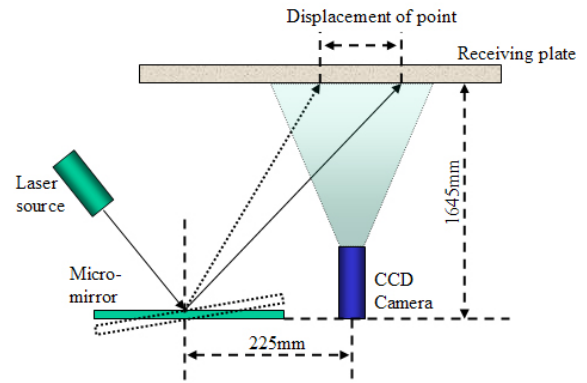
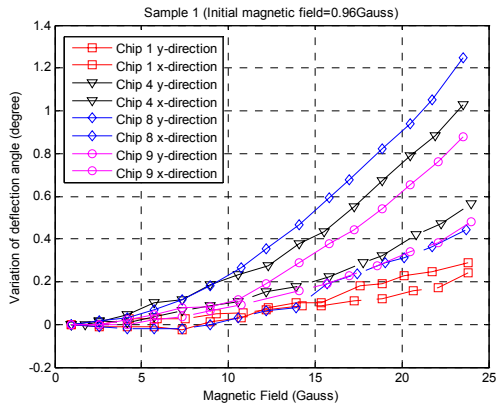
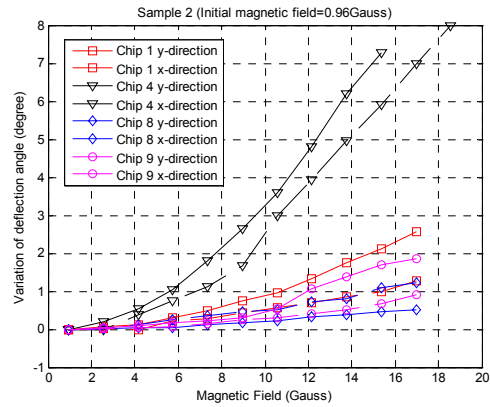


Figure 7 Schematic illustration of laser spot reflection from a MAM

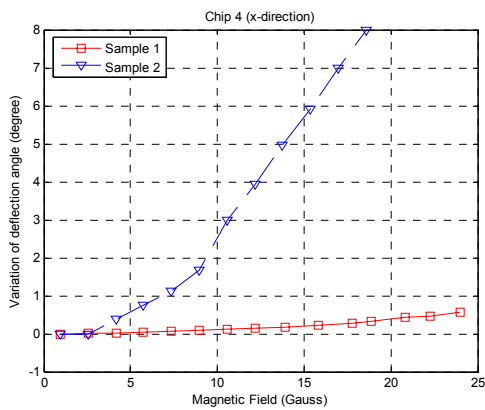


(a)

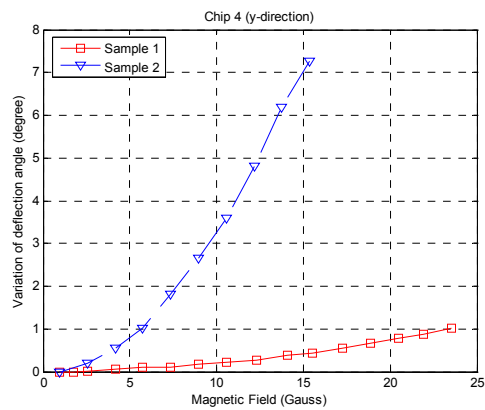


(b)

Figure 8. Deflection angle vs. magnetic field variation (a). for sample 1; (b). for sample 2



(a)



(b)

Figure 9. Deflection angle of MAMs in Chip4 vs. Magnetic field variation (a). x-direction measurement; (b). y-direction measurement